Dynamic Contact Angles and Wetting Front Instability

Christine E. Baver[1], J. Yves Parlange[1], Cathelijne R. Stoof[1],

David A. DiCarlo[2], Rony Wallach[3], and Tammo S. Steenhuis[1*]

[1] Department of Biological and Environmental Engineering, Cornell University, Ithaca, NY 14850, USA.

[2] Department of Petroleum and Geosystems Engineering, University of Texas at Austin, Austin, Texas, 78701, USA

[3] Department of Soil and Water Sciences, The Hebrew University of Jerusalem, Jerusalem, Israel

* Corresponding Author: Tammo Steenhuis, Riley-Robb Hall, Cornell University, Ithaca NY 14853. Email: tss1@cornell.edu

Accepted for publication in WRR.

Abstract

Dynamic contact angles provide a mechanism for initiating the instability of wetting fronts and the formation of fingers/columns in porous media. To study those dynamic contact angles when gravity is present, rectangular capillary tubes were used to facilitate observation of the complete interface without geometric distortion. Results show that if the dynamic contact angle minus the static contact angle is plotted, we can model observations very simply. In addition, we show that in our experiments, contrary to some suggestions, contact angles are independent of capillary size. We also calculate the capillary pressure at the wetting front as a function of the flux of water in the finger and the grain size diameter to explain instability of the front.

Keywords: Dynamic Contact Angle, Instability, Gravity

Running title: Dynamic Contact Angles

1. Introduction

While many experiments have been conducted to study unstable flow, the phenomenon is not fully understood. Early research by Saffman and Taylor [1958] primarily focused on viscous fingering. Experiments of Hill and Parlange [1972] focused instead on gravity fingering, or column flow, where viscosity is less important. Column flow is the most prevalent mechanism in nature to rapidly transport large quantities of water downward, bypassing most of the soil matrix [*Starr et al.*, 1978]. The main difficulty in understanding column flow is that moisture content within these columns is not uniformly distributed (columns are wetter at the tip) and that the wetting takes place only in a few pores. Because Richards' equation assumes that changes take place over the Darcy scale, which is defined as several pores, it cannot be used reliably to estimate derivatives on very few pore distances. Trying to correct Richards' equation by adding higher order derivatives would be even less reliable. Even though Richards' equation cannot be used to analyze processes occurring at the tip of the wetting front, it adequately describes the structure of column flow far enough from the tip. For instance, the decreasing water content with the distance from the tip [*Selker et al.*, 1992] and the width of the column flow [*Parlange and Hill*, 1976] can both be obtained with Richards' equation. While Parlange and Hill [1976] originally assumed that the tip of the column was saturated, this is neither true in general nor necessary [*Hillel and Baker*, 1988; *Liu et al.*, 1995]. An accepted theory to predict the water content at the tip does not exist and therefore in many applications the experimentally observed moisture content is used [*Liu et al.*, 1995]. We suggest that a dynamic contact angle greater than the static contact angle, could provide an explanation for the different observed moisture contents at the wetting front.

2. Hoffman's Shift Factor and Jiang's equation

When dealing with slug flow, four key factors can play a major role: gravity, viscosity, surface tension, and inertia. These factors are quantified using dimensionless numbers. The most important one [*Hoffman*, 1975; *Ngan and Dussan V.*, 1982] is the capillary number (*Ca*) defined as:

$$Ca = \mu v / \gamma \qquad (1)$$

where μ is the viscosity of the liquid (Pa•s), v is a contact line velocity (m/s), and γ is the surface tension (N/m) between the two fluid phases. Hoffman [1975] carried out the first systematic experiment involving the dependence of the dynamic contact angle on velocity using slugs of liquid. Hoffman [1975] performed his experiments with horizontal capillary tubes using a steel plunger and five liquids. Since the tubes were placed horizontally, gravity did not play a role. From two silicon liquids with a static contact angle of zero (GE and Brookfield), Hoffman [1975] plotted dynamic contact angles (ranging from 0 to 180°) as a function of capillary number. Because the dynamic contact angle – capillary number relationships found for other liquids (Dow Corning fluid, Admex and Santicizer) had non-zero static contact angles of 12°, 69° and 67°, respectively, they did not match the initial curve, he then used a "shift" correction to plot the results. This shift factor was found by looking up the capillary number corresponding to the liquid's static contact angle (in the initial curve), and adding this value to the measured capillary values. The resulting graph in which all liquids fit the one curve for θ_s=0 is presented in Fig. S1, in which all points are fitted with an equation introduced by Jiang [1979]:

$$\frac{1-\cos\theta_m}{2} = \tanh(4.96\,Ca^{.702}) \qquad (2)$$

where θ_m is the measured contact angle. For simplicity, Jiang's [1979] curve will be used to depict Hoffman's curve in the rest of the paper, to compare with our results.

3. Materials and Methods

We tested the effect of viscosity and capillary size on dynamic contact angles with gravity effects. 334 experiments were performed with four capillary sizes and five liquids (four silicones and glycerin) in which a liquid slug was allowed to move down a capillary at different inclinations to vary the effect of gravity. For each run, both the velocity of the wetting front and the dynamic contact angle were measured.

3.1 Liquids and capillaries

Experiments were performed with glycerin and different silicon liquids of variable viscosity in different size rectangular capillary tubes. The tubes were 20-60 cm long rectangular borosilicate glass tubes (Friedrich & Dimmock Inc., Millville, NJ, USA) of four different dimensions: 2 x 4 mm, 2 x 6 mm, 3.5 x 9 mm, and 3.85 x 11.95 mm. Five liquids were tested: four silicones (Brookfield Engineering Laboratories Inc., Middleboro, MA, USA) were selected to cover a range of viscosities, and glycerol (*Mallinckrodt,* Paris, KY, USA) (Table 1). The static contact angle of the silicon liquids was 0° in agreement with Hoffman [1975]. The static contact angle of glycerin was measured to be 34° using the static sessile drop method. Viscosity was measured with a SV-10 Vibro Viscometer (Worcestershire, UK); surface tension was measured with a Fisher Surface Tensiomat (Model 21, Fisher Scientific, Pittsburgh, PA, USA) and fluid density was measured by weighing a known volume of liquid.

3.2 Experimental setup

The shape of the moving interface was captured through a Hirox-Digital KH-7700 bright field microscope (Hirox-USA, River Edge, NJ, USA) mounted with a mid-range straight zoom lens (MX-5040SZ) and a low magnification rotary-head adaptor (AD-5040LOWRS), connected to a personal computer (Fig. S2a). Because the microscope had a maximum recording speed of 30 frames/sec, the greatest fluid velocity that could be captured was ~1 cm/s. Results were obtained with recording speeds between 30 frames/sec and 20 frames/min, depending on the velocity of the liquid. To vary the strength of gravitational force, a platform with an adjustable apparatus was designed to support capillary tubes at different fixed inclinations (Fig. S2b). A built-in protractor, made of thick transparent acrylic, allowed the apparatus to be adjusted for inclinations between 0° and 90°, while a small piece of paper placed on the apparatus arm provided a white background and reduced light reflection or image distortion from the acrylic material. The setup was designed such that air could move freely at both ends of the capillary. To allow for microscope images be taken at a 90° angle with the capillary, the microscope was tilted to offset the inclination of the capillary tube (Fig. S2c).

3.3 Experimental procedure

At the start of each experiment, a slug of liquid between 150 and 3000 µl was pipetted into a horizontally-placed capillary tube. The slugs were long enough to ensure that the velocity once constant follow Poiseuille’s law. The two ends of the tube were then capped to minimize premature sliding of the liquid as it was placed on the apparatus. At the desired inclination, the slug was then allowed to move down the tube. After an initial transition period, when the wetting front had traveled 2-5 cm down the tube and velocity became constant, images were taken for contact angle and velocity analysis. Capillary tubes were cleaned between runs (Text S1) and used multiple times throughout the experiment.

3.4 Image analysis

Velocity and dynamic contact angle was determined using ImageJ (US National Institute of Mental Health). To account for the index of refraction, all velocity and radius measurements were adjusted by a factor of 0.93 following Hoffman [1975]. Velocity was determined by locating the pixel position of the meniscus on a series of subsequent images, and noting the time that the image was recorded. The slug velocity was then calculated as Δpixels/Δtime and converted to m/s using the appropriate image resolution. Contact angles were determined using two methods:

1) For the protractor measurements [*Hoffman*, 1975], images of dynamic menisci were enlarged and lines were drawn on the liquid-solid-interface (XY in Fig. S3a), and the liquid-air interface (YZ). The contact angle was then calculated by an ImageJ function, and the procedure repeated for the other side. Because the apparatus was not always perfectly level, left and right contact angles were averaged before further analyses. If left and right contact angles differed by more than 5° due to too much tilting of the chamber, the run was discarded. For angles between 60°-120° we found that the interface was consistently circular and the protractor method was adequate for contact angle analysis. Angles above 140° are not included in the analysis since they could not be measured very accurately.

2) The apex-contact line method (Fig S3b) of Ngan and Dussan [1982] was also used for data above 120°. Data were only used after verifying that the contact line was circular, as this method assumes that the interface contact line is the arc of a circle. We found that the protractor method was more subjective at high and low contact angles, as pointed out by Ngan and Dussan [1982].

4. Results and Discussion

4.1 Relationship between Froude and Reynolds number

To verify whether Poiseuille's Law applied to the experimental runs, the Froude number was plotted against the Reynolds' number (Eq. 4, Fig. 1) for each run (n=334 for 12 liquid/chamber size combinations; Table S1).

$$\frac{Fr}{Re} = \frac{\frac{inertia}{gravity}}{\frac{inertia}{viscosity}} = \frac{viscosity}{gravity} = \frac{\mu v}{\rho g r^2} \quad (4)$$

The linear relationship between Froude and Reynolds' number shown for the red squares in Fig. 1 indicates that Poiseuille's Law applies because the slugs were sufficiently long. This is the case when the flow at the tip and end of slug has negligible impact. The few points deviating from this line (blue diamonds) were done with shorter slugs at low inclinations to show that Poiseuille's Law does not apply, meaning that end effects are important.

Fig. 2a shows the measured dynamic contact angles plotted against their capillary number. Although there is considerable scatter between the various liquid/chamber size combinations, the general pattern is that as wetting speed increases, dynamic contact angles increase very much as observed by Hoffman [1975]. Applying Hoffman's shift (Section 2) to reduce scatter barely improved the R^2 value, from 0.63 to 0.67.

Instead, we introduce the reduced contact angle (θ_r) defined as

$$\theta_r = \frac{\theta_m - \theta_s}{(180 - \theta_s)} * 180 \quad (5)$$

where θ_s is that static contact angle. Plotting the dynamic contact angle-capillary number data using this reduced contact angle gives us an R^2 of 0.86 (Fig 2b). Comparison of Hoffman [1975] curve and our fitted line curve of our reduced contact angle shows they are very close. Only at lower capillary numbers, out contact angles were slightly greater than Hoffman. This could possibly be due to the rectangular geometry instead of the cylindrical tube used in Hoffman's experiments.

4.2 Size effects

Some researchers [*Ngan and Dussan V.*, 1982; *Legait and Sourieau*, 1985] propose that with larger size, dynamic contact angle increases. In our experiments with 2x4 mm and 2x6 mm chambers, circular interfaces were observed and contact angles were not affected by size. However, for larger capillary tubes (3.5 x 9 mm, 3.85-11.95 mm) asymmetric contact lines and non-circular interfaces (Table S2) were observed. In that case, a protractor is used to measure the angle at the inflection point. The apex-contact line method cannot be used or it would lead to an overestimation of the dynamic contact angle due to incorrectly assuming a circular interface (Fig 3). Altogether, we find no correlation of dynamic contact angle and capillary size. It is interesting that Ngan and Dussan [1982] had lower dynamic contact angles than Hoffman for smaller dimensions, their results for larger dimensions were actually closer to Hoffman.

4.3 Instability

We now relate dynamic contact angles to instability of wetting fronts in soil. It is immediately clear that for average water fluxes in soil during natural infiltration of 0.1-10 cm/h (related capillary numbers of 2 x 10^{-7} to 2 x 10^{-5}) the dynamic contact angle would be hardly different from the static contact angle. At the same time it is obvious that "average water flux" does not exist in the pores and necks in a finger/column at the wetting front. Assuming that only one meniscus breaks through at the finger tip at one time requires a high velocity and a high pressure (the pressure overshoot measured by Selker *et al.* [1992b] and DiCarlo [2007]). Immediately after the water leaves a pore neck, the pressure drops and then build up again until the water breaks through in another neck. Thus water flows through one pore at the time at the wetting front. We saw this phenomenon where one pore "pops" at a time during imbibition from the bottom (with much lower velocities than wetting fronts) in a 1 cm thick light chamber (see also Fig. 8 in *Selker et al.*, 1992b).

When we apply this principle to the fingered flow experiments of *Glass et al.* [1989], where for a typical 1.5 cm-wide finger in a 1 cm x 80 chamber cross section with sand sizes of around 0.4 mm, the flux in the finger is approximately 10 cm^3/min. Assuming that this flux has to go through a pore neck with a radius of 0.21 mm results in a velocity in the pore neck of approximately 1.2 m/sec with capillary number of 0.015 and a dynamic contact angle of 60° according to Hoffman's and our results. This 60° angle explains why water infiltrates in the soil at less negative pressure (approximately 3.5 cm for *Glass et al.* [1989], also measured by *Selker et al.* [1992b]) than postulated by Richards's equation that assumes a static contact angle. In conclusion, effects of velocity on the value of the dynamic contact angles at the wetting front is providing a mechanism for increasing pressure at the wetting front which is necessary for wetting front instabilities in soils.

5. Conclusions

In conclusion, using rectangular capillaries allows us to view interfaces without distortion, however the geometry of the capillary may be responsible for very slight differences between our and Hoffman's [1975] results for θ_s=0. We found that using a reduced dynamic contact angle simplifies the presentation of the dynamic contact angle-capillary number relationship. We found circular interfaces in smaller diameter chambers but as the capillary size increased, eventually interfaces began to deviate from a circular meniscus and in that case the dynamic contact angle can be measured with a protractor. Capillary size had no measureable impact on dynamic contact angles. Finally, dynamic contact angles can explain the increased pressure at the wetting front and hence the instability observed in finger experiments.

Acknowledgments

We wish to thank Doug Caveney for building the adjustable apparatus. This study was financed by the Binational Agricultural Research and Development Fund (BARD), Project No. IS-3962-07.

References

DiCarlo, D. A. (2007), Capillary pressure overshoot as a function of imbibition flux and initial water content, *Water Resour. Res.*, *43*(8), W08402, doi:10.1029/2006WR005550.

Glass, R. J., T. S. Steenhuis, and J.-Y. Parlange (1989), Wetting front instability: 2. Experimental determination of relationships between system parameters and two-dimensional unstable flow field behavior in initially dry porous media, *Water Resources Research*, *25*(6), 1195–1207, doi:10.1029/WR025i006p01195.

Hill, D. E., and J.-Y. Parlange (1972), Wetting Front Instability in Layered Soils, *Soil Science Society of America Journal*, *36*(5), 697–702, doi:10.2136/sssaj1972.03615995003600050010x.

Hillel, D., and R. S. Baker (1988), A DESCRIPTIVE THEORY OF FINGERING DURING INFILTRATION INTO LAYERED SOILS, *Soil Science*, *146*(1), 51–56, doi:10.1097/00010694-198807000-00008.

Hoffman, R. L. (1975), A study of the advancing interface. I. Interface shape in liquid—gas systems, *Journal of Colloid and Interface Science*, *50*(2), 228–241, doi:10.1016/0021-9797(75)90225-8.

Jiang, T.-S., O. . Soo-Gun, and J. C. Slattery (1979), Correlation for dynamic contact angle, *Journal of Colloid and Interface Science*, *69*(1), 74–77, doi:10.1016/0021-9797(79)90081-X.

Legait, B., and P. Sourieau (1985), Effect of geometry on advancing contact angles in fine capillaries, *Journal of Colloid and Interface Science*, *107*(1), 14–20, doi:10.1016/0021-9797(85)90144-4.

Liu, Y., J.-Y. Parlange, T. S. Steenhuis, and R. Haverkamp (1995), A Soil Water Hysteresis Model for Fingered Flow Data, *Water Resources Research*, *31*(9), 2263, doi:10.1029/95WR01649.

Ngan, C. G., and E. B. Dussan V. (1982), On the Nature of the Dynamic Contact Angle: An Experimental Study, *Journal of Fluid Mechanics*, *118*, 27–40, doi:10.1017/S0022112082000949.

Parlange, J.-Y., and D. Hill (1976), Theoretical Analysis of Wetting Frong Instability in Soils, *Soil Science October 1976*, *122*(4), 236–239.

Saffman, P. G., and G. Taylor (1958), The Penetration of a Fluid into a Porous Medium or Hele-Shaw Cell Containing a More Viscous Liquid, *Proc. R. Soc. Lond. A*, *245*(1242), 312–329, doi:10.1098/rspa.1958.0085.

Selker, J. S., T. S. Steenhuis, and J.-Y. Parlange (1992a), Wetting Front Instability in Homogeneous Sandy Soils under Continuous Infiltration, *Soil Science Society of America Journal*, *56*(5), 1346–1350, doi:10.2136/sssaj1992.03615995005600050003x.

Selker, J. S., J.-Y. Parlange, and T. S. Steenhuis (1992b), Fingered Flow in Two Dimensions 2. Predicting Finger Moisture Content, *Soil Science Society of America Journal*, *28*(9), 2523–2528.

Starr, J. L., H. C. DeRoo, C. R. Frink, and J.-Y. Parlange (1978), Leaching Characteristics of a Layered Field Soil, *Soil Science Society of America Journal*, *42*(3), 386–391, doi:10.2136/sssaj1978.03615995004200030002x.

Table 1: Summary of Liquid Properties. Values are averages over the replicates of the measurement (n=3) ± one standard deviation.

Manufacturer	Liquid	Viscosity (Pa•s)	Surface tension (N/m)	Density (kg/m^3)	Static contact angle (°)
Dow Corning	Glycerin	1.34±0	0.0640±0.002	1254±4	34±3
Brookfield Standard	V100000	104.32*	0.0225±0.002	999±4	0
Brookfield Standard	V30000	30.88*	0.0226±0.002	1002±15	0
Brookfield Standard	V500	0.486*	0.0240±0.002	975±12	0
Brookfield Standard	V100	0.0968*	0.0227±0.002	966±4	0

*supplied by manufacturer

Figure S1: Hoffman's [1975] experimental data (points) with the fitted approximation by Jiang [1979] (line).

Figure S2a): Experimental setup comprising of adjustable apparatus stand with a capillary tube (A), see detail in S2b), mounted on a stand (B), and a bright-field microscope (C) connected to a personal computer that displays the image (D). Adjustable apparatus stand (2b, 2c) is composed of a platform with an adjustable arm (F) which position can be changed and fixed to a required inclination using a thumb screw (G) and a protractor or inclination scale (H) mounted behind the adjustable arm.

Figure S3a) Protractor method measurement of contact angle (θ_a) in a capillary, with lines drawn (XYZ) for calculation of the contact angle; and 3b) apex method of measuring contact angle that uses the Cartesian coordinate values of the point where the liquid, capillary tube and air meet (A, B) and the position where the liquid and air intersect at the radius of the capillary (C). Figure S3b is adjusted from Bian [2004].

Figure 1: Froude vs. Reynolds Number (n=334) for 5 different liquids and 4 chamber sizes in which red squares indicate experimental results that followed Poiseuille's Law, and blue diamonds that did not. A linear regression line is fitted (R^2=0.99).

Figure 2: a) All experimental results plotted with dynamic contact angle as a function of capillary number. Jiang's [1979] gives an $R^2 = 0.63$, b) All experimental results plotted with a reduced dynamic contact angles; $\theta_{\text{Reduced}} = \frac{\theta_m - \theta_s}{(180 - \theta_s)} * 180$ as a function of capillary number; R^2=0.86 using a best fit curve.

Figure 3: Comparison of protractor method on non-circular interfaces, measuring that angle at the inflection point and the apex-contact line method. The latter is not applicable for such an interface. Image A is a 3.5-9 mm chamber, image B is 3.85-11.95 mm chamber.

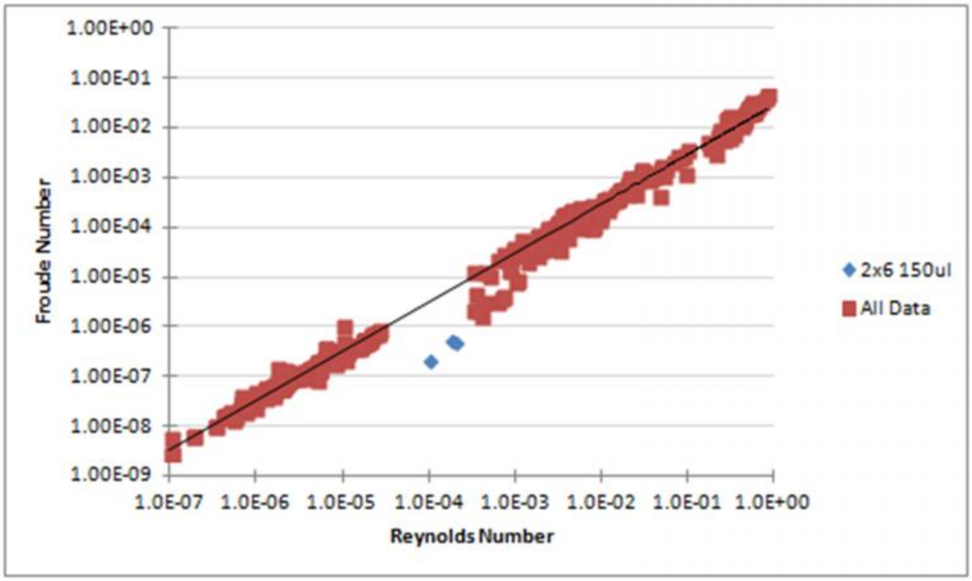
1.00E+00
1.00E-01
1.00E-02
1.00E-03
1.00E-04
1.00E-05
1.00E-06
1.00E-07
1.00E-08
1.00E-09
Froude Number
1.0E-07
1.0E-06
1.0E-05
1.0E-04
1.0E-03
1.0E-02
1.0E-01
1.0E+00
Reynolds Number
2x6 150ul
All Data

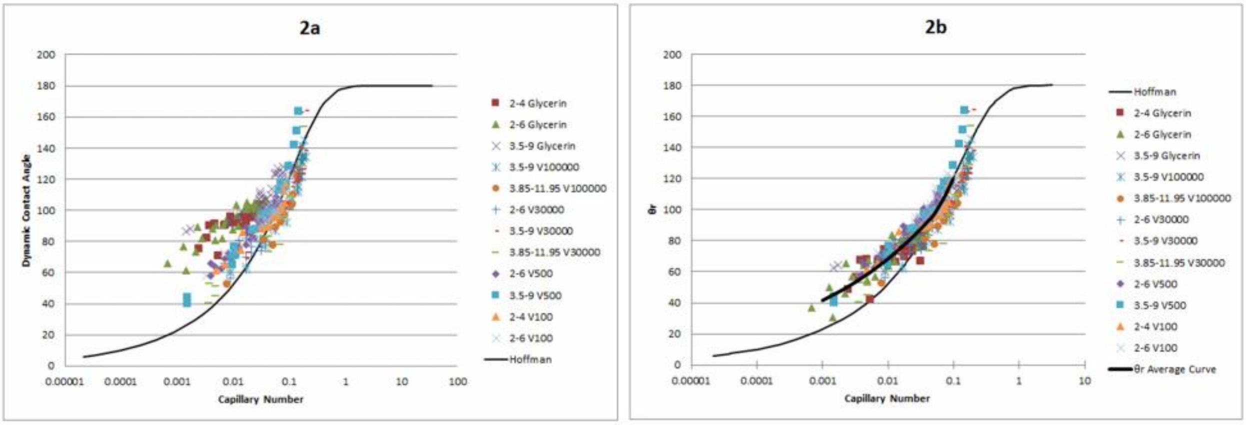
2a
Dynamic Contact Angle
Capillary Number
2-4 Glycerin
2-6 Glycerin
3.5-9 Glycerin
3.5-9 V100000
3.85-11.95 V100000
2-6 V30000
3.5-9 V30000
3.85-11.95 V30000
2-6 V500
3.5-9 V500
2-4 V100
2-6 V100
Hoffman
2b
θr
Capillary Number
Hoffman
2-4 Glycerin
2-6 Glycerin
3.5-9 Glycerin
3.5-9 V100000
3.85-11.95 V100000
2-6 V30000
3.5-9 V30000
3.85-11.95 V30000
2-6 V500
3.5-9 V500
2-4 V100
2-6 V100
θr Average Curve

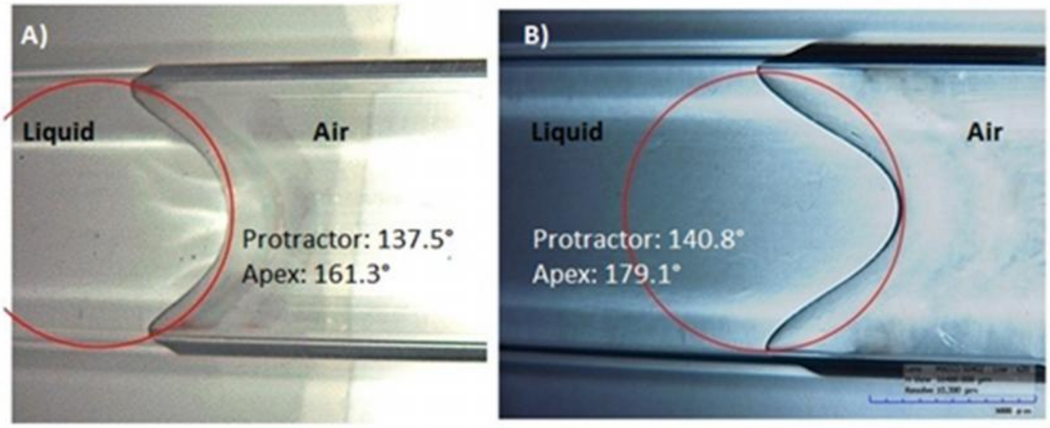
A)
Liquid
Air
Protractor: 137.5°
Apex: 161.3°
B)
Liquid
Air
Protractor: 140.8°
Apex: 179.1°

Supplementary material

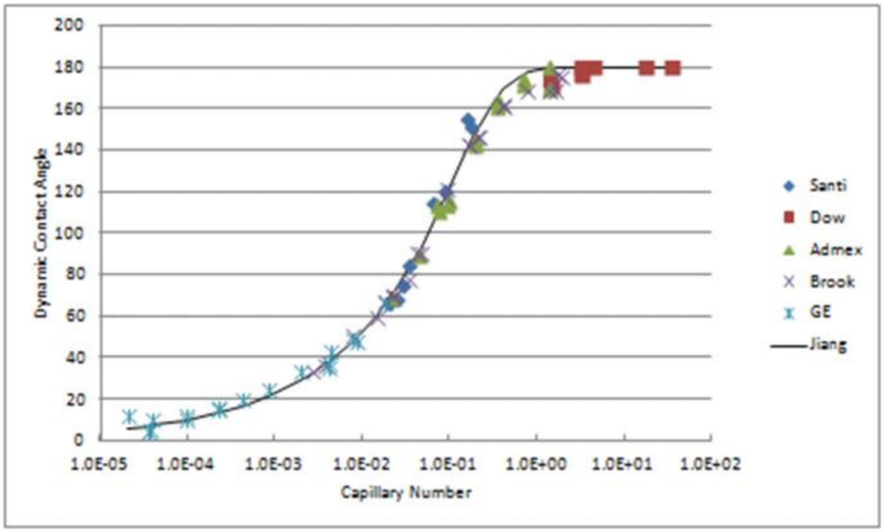

Figure S1

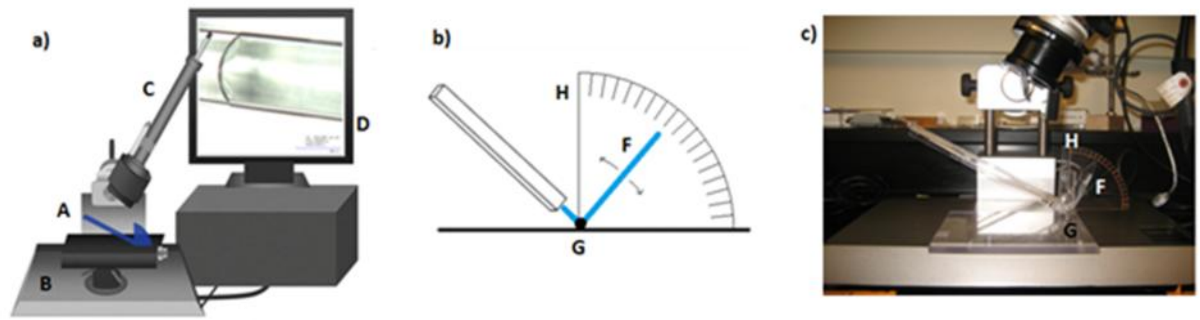

Figure S2

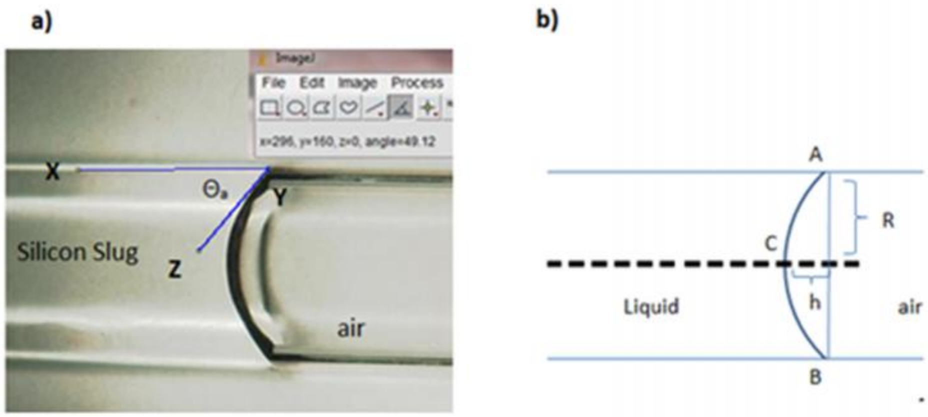
a)
ImageJ
File Edit Image Process
x=296, y=160, z=0, angle=49.12
X
Θa
Y
Silicon Slug
Z
air
b)
A
R
C
Liquid
h
air
B

Figure S3